NASA/TM—2001-211306

Effect of Microstructure on Creep in Directionally Solidified NiAl-31Cr-3Mo

J.D. Whittenberger and S.V. Raj
Glenn Research Center, Cleveland, Ohio

I.E. Locci
Case Western Reserve University, Cleveland, Ohio

December 2001

The NASA STI Program Office . . . in Profile

Since its founding, NASA has been dedicated to the advancement of aeronautics and space science. The NASA Scientific and Technical Information (STI) Program Office plays a key part in helping NASA maintain this important role.

The NASA STI Program Office is operated by Langley Research Center, the Lead Center for NASA's scientific and technical information. The NASA STI Program Office provides access to the NASA STI Database, the largest collection of aeronautical and space science STI in the world. The Program Office is also NASA's institutional mechanism for disseminating the results of its research and development activities. These results are published by NASA in the NASA STI Report Series, which includes the following report types:

- TECHNICAL PUBLICATION. Reports of completed research or a major significant phase of research that present the results of NASA programs and include extensive data or theoretical analysis. Includes compilations of significant scientific and technical data and information deemed to be of continuing reference value. NASA's counterpart of peer-reviewed formal professional papers but has less stringent limitations on manuscript length and extent of graphic presentations.

- TECHNICAL MEMORANDUM. Scientific and technical findings that are preliminary or of specialized interest, e.g., quick release reports, working papers, and bibliographies that contain minimal annotation. Does not contain extensive analysis.

- CONTRACTOR REPORT. Scientific and technical findings by NASA-sponsored contractors and grantees.

- CONFERENCE PUBLICATION. Collected papers from scientific and technical conferences, symposia, seminars, or other meetings sponsored or cosponsored by NASA.

- SPECIAL PUBLICATION. Scientific, technical, or historical information from NASA programs, projects, and missions, often concerned with subjects having substantial public interest.

- TECHNICAL TRANSLATION. English-language translations of foreign scientific and technical material pertinent to NASA's mission.

Specialized services that complement the STI Program Office's diverse offerings include creating custom thesauri, building customized data bases, organizing and publishing research results . . . even providing videos.

For more information about the NASA STI Program Office, see the following:

- Access the NASA STI Program Home Page at ***http://www.sti.nasa.gov***

- E-mail your question via the Internet to help@sti.nasa.gov

- Fax your question to the NASA Access Help Desk at 301–621–0134

- Telephone the NASA Access Help Desk at 301–621–0390

- Write to:
  NASA Access Help Desk
  NASA Center for AeroSpace Information
  7121 Standard Drive
  Hanover, MD 21076

NASA/TM—2001-211306

Effect of Microstructure on Creep in Directionally Solidified NiAl-31Cr-3Mo

J.D. Whittenberger and S.V. Raj
Glenn Research Center, Cleveland, Ohio

I.E. Locci
Case Western Reserve University, Cleveland, Ohio

Prepared for the
131st Annual Meeting and Exhibition
sponsored by the Minerals, Metals, and Materials Society
Seattle, Washington, February 17–21, 2002

National Aeronautics and
Space Administration

Glenn Research Center

December 2001

Available from

NASA Center for Aerospace Information
7121 Standard Drive
Hanover, MD 21076

National Technical Information Service
5285 Port Royal Road
Springfield, VA 22100

Available electronically at http://gltrs.grc.nasa.gov/GLTRS

EFFECT OF MICROSTRUCTURE ON CREEP IN DIRECTIONALLY SOLIDIFIED NiAl-31Cr-3Mo

J.D. Whittenberger and S.V. Raj
National Aeronautics and Space Administration
Glenn Research Center
Cleveland, Ohio 44135

I.E. Locci
Case Western Reserve University
Cleveland, Ohio 44106

SUMMARY

The 1200 to 1400 K slow strain rate characteristics of the directionally solidified (DS) eutectic Ni-33Al-31Cr-3Mo have been determined as a function of growth rate. While differences in the light optical level microstructure were observed in alloys grown at rates ranging from 7.6 to 508 mm/h, compression testing indicated that all had essentially the same strength. The exception was Ni-33Al-31Cr-3Mo DS at 25.4 mm/h which was slightly stronger than the other growth velocities; no microstructual reason could be found for this improvement. Comparison of the ~1300 K properties revealed that four different DS NiAl-34(Cr,Mo) alloys have a similar creep resistance which suggests that there is a common, but yet unknown, strengthening mechanism.

INTRODUCTION

Directionally solidified (DS) systems based on the NiAl-34(at.%) Cr eutectic are under consideration as possible replacements for Ni-based superalloys exposed to severe temperature, stress, and environment conditions. The unique microstructures created during directional solidification, in the form of aligned ~1 μm diameter Cr fibers in a NiAl matrix for NiAl-34Cr (ref. 1) or aligned micron thick alternating NiAl and α-(Cr,Mo) lamella in NiAl-(34-x) -xMo (x > 0. 6 percent) (ref. 2), result in both good elevated temperature creep strength and reasonable room temperature toughness (refs. 3 to 9). In particular the improvement in creep properties is remarkable compared to those of the constituents: for example the 1300 K – $10^{-7}s^{-1}$ strength of DS NiAl-34Cr is about 100 MPa (ref. 3); whereas polycrystalline NiAl (ref. 10), [100]-oriented NiAl single crystals (refs. 3 and 11) and large grain size Cr (refs. 12 and 13) would require only 10 to 15 MPa to deform at these conditions.

Since the early work by Cline and Walter (ref. 2) did not report a clear dependency between the "goodness" of alignment and mechanical properties for NiAl-34Cr based eutectics, NiAl-31Cr-3Mo was DS at rates ranging from 12.7 to 508 mm/h and subjected to both room temperature toughness and elevated temperature slow strain rate compressive testing (ref. 6). The initial results indicated that 1200 and 1300 K strength properties were similar for all the growth rates. This paper extends the preliminary study on the elevated temperature properties of DS NiAl-31Cr-3Mo as a function of growth rate to include an as-cast alloy, a very slowly grown eutectic (7.6 mm/h), testing at 1400 K, and a few constant load creep experiments to achieve slower strain rates. The strength properties of DS NiAl-31Cr-3Mo are examined in light of the available microstructural data and are compared to those for other NiAl-34Cr based eutectics. Lastly, potential mechanisms responsible for the high strength of DS NiAl-(Cr,Mo) eutectics are examined.

EXPERIMENTAL PROCEDURES

The methods used for casting the prealloyed NiAl-31Cr-3Mo rods and for directionally solidification to produced aligned eutectic bars at growth rates ranging from 7.6 to 508 mm/h are completely discussed in (refs. 6, 7, and 14). Since the original bar grown at 7.6 mm/h in ref. 6 was significantly off chemistry (28.6Al instead of 33Al), a new bar was DS at this rate utilizing an as-cast rod with the correct composition. Compression specimens were

taken from the aligned region of each DS bar by wire electrodischarge machining (EDM). The compression specimens were 8 by 4 by 4 mm in size with the 8 mm sample length parallel to the growth axis, and they were tested in the as-EDM'ed surface condition. A set of compression samples was also machined from an as-cast rod (the one partially utilized for the DS run at 12.7 mm/h) in order to access the strength improvement from directional solidification; the long axis of these samples was parallel to the length of the casting.

Elevated temperature compressive strength properties were mainly determined by constant velocity testing which was supplemented with a few constant load creep tests. A screw driven universal testing machine was utilized for constant velocity testing, where samples were compressed between two solid push bars at 1200 to 1400 K in air at crosshead rates that varied from 1.7×10^{-2} to 1.6×10^{-6} mm/s. The autographically recorded load–time curves were converted to true stresses, strains and strain rates via the offset method in combination with a normalization to the final specimen length and the assumption of a constant volume. Constant load compressive creep experiments were undertaken in a lever arm creep machine, where time dependent deformation was determined by measurement of the relative positions of the ceramic push bars applying the load to the specimen. All the contraction–time data from creep testing were normalized with respect to the final specimen length and converted into true stresses and strains assuming that the sample volume was constant.

RESULTS

Materials

Characterization of the chemistry of the individual as-cast rods and DS bars are reported in (refs. 6, 7, and 14), and the compositional control was very good. Grouping all the bars DS between 7.6 and 508 mm/h together, the average composition was Ni-33.4Al-31.2Cr-2.9Mo with standard deviations of 0.6 at.% for Al and Cr, and 0.1 percent for Mo; each bar also contained about 0.14 percent Si and small amounts of C (~0.06 percent), N (~0.001 percent) and O (~0.02 percent). The as-cast rod, which was compression tested in this study, had the following composition: Ni-33.3Al-31.1Cr-3.0Mo with 0.013Si-0.07C-0.007N and 0.07O. The higher Si content in the DS rods in comparison to the as-cast bars is probably the result of long exposures during solidification in crucibles which contained a SiO_2 binder.

Transverse microstructural sections of the DS rods illustrated that large diameter lamellar eutectic grains with sharp boundaries formed (fig. 1(a)) at and below growth rates of 12.7 mm/h, while at higher velocities ~200 μm diameter cellular structures bounded by relatively thick intercellular regions developed (fig. 1(b)). The lamellar eutectic grains were composed of alternating NiAl and α-(Cr,Mo) plates while the cells contained lamellae in a radial-like pattern which some cases terminated and in other cases coarsened to form the intercellular regions. The as-cast microstructure transverse to the casting direction is illustrated in figure 1(c), where cells containing a fine pearlitic structure were surrounded by relatively wide intercellular regions. Examination of longitudinal sections of the DS rods (refs. 6 and 14) indicated that both the lamellar eutectic grains and cellular grains were mm's in length; however the lamellae were not always parallel to the growth direction. Additional details about the microstructures of DS NiAl-31Cr-3Mo as a function of growth rate are given in (ref. 6) and extensive quantitative measurements are presented in (ref. 14).

Compressive Properties

Examples of the true compressive stress–strain diagrams from 1300 K constant velocity testing of Ni-33Al-31Cr-3Mo are presented in figure 2 as a function of nominal strain rate. The curves for as-cast samples (fig. 2(a)) are similar in appearance at each imposed strain rate, where, in general, rapid work hardening occurred through ~1 percent strain and is followed by continued deformation at a more or less constant flow stress. The stress–strain diagrams for specimens taken from the bar grown at 12.7 mm/h (fig. 2(b)) are similar to those for the as-cast alloy except they tend to exhibit slow strain softening after reaching a maximum stress. In terms of general behavior figure 2 illustrates that strength decreases with decreasing strain rate, the compressive properties are reproducible (i.e., two tests at ~$2\times10^{-7}s^{-1}$, fig. 2(b)), and at any strain rate the DS version is stronger than the as-cast alloy. Testing of all the directionally solidified bars of Ni-33Al-31Cr-3Mo between 1200 and 1400 K and the as-cast alloy at 1200 and 1400 K produced stress–strain curves similar to those shown in figure 2. A number of additional stress–strain curves for directionally solidified materials as a function of growth rate are given in (ref. 6).

Typical 1300 and 1400 K constant load compressive creep curves for a directionally solidified alloy are presented in figure 3. On initial loading the specimens displayed normal primary creep, where the instantaneous deformation rate decreased with time, until steady state creep was established. As illustrated in this figure, several directionally solidified samples were step loaded to higher stress levels during testing. While only a few samples were studied in this manner, step loading did not lead to a normal primary creep response. Invariably after a load increase, the directionally solidified samples transitioned almost immediately into steady state creep which eventually lead to tertiary creep.

True flow stress (σ)–strain rate ($\dot{\varepsilon}$) behavior for the as-cast Ni-33Al-31Cr-3Mo (solid circles) and all the directionally solidified bars are presented in figure 4 as a function of temperature (T). In these plots the flow stresses taken from constant velocity testing are represented by the stress at 1 percent strain from the stress–strain curves (fig. 2), while the flow stresses from creep testing are arithmetic averages calculated over the steady state regimes (fig. 3). By visual inspection the data in figures 4(a) to (c) indicate that directional solidification of Ni-33Al-31Cr-3Mo between 7.6 and 508 mm/h provides a clear strength advantage over simple casting between 1200 and 1400 K. Furthermore, with the exception of the weakness at faster strain rates (1200/1300 K > $10^{-5}s^{-1}$; 1400 K > $10^{-3}s^{-1}$) displayed by the eutectic grown at 7.6 mm/h, the elevated temperature strength properties of DS Ni-33Al-31Cr-3Mo do not appear to be strongly dependent on growth rate.

Examples of the temperature dependence of the true flow stress–strain rate results for the as-cast and DS alloys are illustrated in figure 5. While the as-cast alloy (fig. 5(a)) displayed linear behavior over the entire test range in a stress–logarithm strain rate format, only portions of the flow stress–strain rate–temperature data for the directionally solidified versions could be linearized by either a stress–logarithm strain rate format (fig. 5(b)) or a logarithm stress–logarithm strain rate format (fig. 5(c)). As shown in figure 5(b), the semilogarithm plot tends to successfully portray the faster, lower temperature results, but it fails to account for the higher temperature, slower strain rate tests (i.e., the 1400 K creep data, fig. 5(b)). The logarithm–logarithm format (fig. 5(c)), on the other hand, is capable of accounting for the slower, high temperature creep results but not the faster, lower temperature data.

Where appropriate, the σ-$\dot{\varepsilon}$-T data for all the alloys were fitted by linear regression techniques to either a temperature-compensated exponential law

$$\dot{\varepsilon} = A \exp(C\sigma)\exp(-Q/(RT)), \tag{1}$$

or a temperature-compensated power law,

$$\dot{\varepsilon} = A \sigma^{n}\exp(-Q/(RT)), \tag{2}$$

where A is a constant, C is the stress constant, n is the stress exponent, Q is the activation energy for deformation and R is the universal gas constant. The values for A, C, n, Q and the standard deviations for the stress constant (δ_C), stress exponent (δ_n) and activation energy (δ_Q) as well as the coefficient of determination (R_d^2) for each fit are given in table I. In addition this table notes which data points were not used in these regression analyses. The calculated fits for the as-cast alloy and Ni-33Al-31Cr-3Mo DS at 50.8 mm/h are presented as curves in figures 5(a) to (c) respectively. These lines illustrate the valid range for each regression equation, and they visibly show the good ability of either equations (1) or (2) to describe the data which is confirmed by the relatively high R_d^2 values (>0.96) for each fit in table I.

Although either equations (1) and (2) can describe the data for each material condition, examination of the fit parameters for Ni-33Al-31Cr-3Mo DS at rates from 12.7 to 508 mm/h show a wide range in values even though all six alloys possess similar strengths at each test temperature (fig. 4). For example from the temperature-compensated exponential law fits the stress constants vary from 0.0294 to 0.0363 and the activation energies from –452 to –582 kJ/mol; likewise from the temperature-compensated power law analyses n ranges from 4.43 to 5.61 and Q from –405 to –540 kJ/mol. Because of the similarity of strength among the versions of DS Ni-33Al-31Cr-3Mo, this large range in descriptive parameters is probably an artifact of the least squares approach.

To determine if any one directional solidification growth rate had a strength advantage, the individual sets of data were tested against each other employing a dummy variable in a multiple linear regression analyses. Because interest in DS Ni-33Al-31Cr-3Mo is mainly directed toward its slow creep behavior, this analysis was based on that range of data which could be successfully described by the temperature compensated power law (eq. (2)). To this end, appropriate data from two growth rates were initially tested for a difference; if no difference was found, the sets were joined and tested against flow stress–strain rate–temperature results for another growth rate. When a difference was found, this group of data was set aside until all seven growth rates were tested. Finally the joined set of data was retested against those perceived to be different to determine if the discrepancy was persistent.

The results from the statistical analyses to differentiate 1200 to 1400 K creep strength on the basis of directional solidification growth rate are shown in figure 6. In the temperature compensated power law regime six of the seven DS rates (7.6, 12.7, 50.8, 127, 254 and 508 mm/h, open symbols in fig. (6)) possessed 1200 to 1400 K compressive properties which could not be separated from one another, where

$$\dot{\varepsilon} = 1000\,\sigma^{4.99}\exp(-487.3/(RT)) \quad (3)$$

The solid curves in figure 6 illustrate the fit of equation (3), and they can be compared to the behavior of Ni-33Al-31Cr-3Mo DS at 25.4 mm/h (solid symbols) which demonstrates a small strength advantage over the other six growth conditions. While the behavior of the 25.4 mm/h alloy is accurately characterized by n = 5.61 and Q = –539.4 kJ/mol ($R_d^2 = 0.991$, table I), use of a dummy variable can force a fit to have the same stress exponent and activation energy as equation (3). Thus the behavior of Ni-33Al-31Cr-3Mo DS at 25.4 mm/h can be reflected by a lower pre-exponent term, where

$$\dot{\varepsilon} = 519\,\sigma^{4.99}\exp(-487.3/(RT)) \quad (4)$$

which corresponds to an ~14 percent strength advantage, as illustrated by the dashed lines in figure 6 which closely reproduce the experimental results. Taken together equations (3) and (4) are able to describe the temperature compensated power law characteristics of Ni-33Al-31Cr-3Mo directionally solidified over a 60 fold range in growth rates with a R_d^2 of 0.947 and $\delta_n = 0.14$ and $\delta_Q = 18.1$ kJ/mol.

DISCUSSION

Over the current range in testing (figs. 4 and 6) the 1200 to 1400 K strength of Ni-33Al-31Cr-3Mo DS at 25.4 mm/h is statistically slightly better than that observed for slower or faster growth rates. Comparison of this improvement to the detailed microstructural measurements made on transverse sections by Raj and Locci (ref. 14) and the estimates of the minimum grain/cell length in the longitudinal/DS growth direction (fig. 7) do not reveal any obvious microstructural feature responsible for the increase. Neither the minimum grain/cell length, average cell diameter, intercellular region width (area fraction), interlamellar spacing nor NiAl lamella width for the alloy grown at 25.4 mm/h display any characteristic which separates it from other DS rates. Thus, the reason for the additional strength of the alloy grown at 25.4 mm/h is not known; most certainly, if there is further interest in this alloy system, more bars should be directionally solidified at this velocity and tested to confirm the current behavior.

With regard to the elevated temperature strength of NiAl-31Cr-3Mo, the 1200 to 1400 K compressive data in figure 4 indicate that directional solidification does produce a significant strength increase compared to simple casting. Furthermore, as illustrated by the 1273 K creep data in figure 8, directional solidification of NiAl-34Cr and NiAl-33Cr-1Mo (ref. 4) vastly improves the properties in comparison to single- (ref. 11) and poly- (ref. 10) crystalline NiAl, polycrystalline Cr (refs. 12 and 13) or a powder metallurgy processed very small grain size NiAl (157 or 10 μm) containing 27 at.% Cr in the form of 1.7 or 3.5 μm particles (ref. 15). While the results in figures 4 and 8, as well those for other NiAl-34Cr eutectics with or without Mo additions (refs. 3 to 9), demonstrate that directional solidification is effective, the mechanism(s) for improvement are not clear. Figure 9 illustrates the compressive properties for several DS NiAl-(Cr,Mo) alloys at/near 1300 K, and, even though the individual stress exponents range from ~5.6 to 8.2, the overall behavior suggests that, to a good first approximation, directionally solidified NiAl-34Cr, NiAl-33Cr-1Mo, NiAl-31Cr-3Mo and NiAl-28Cr-6Mo all possess equivalent strengths. Thus, while there are many significant differences among these DS eutectics,[1–4] it appears that strengthening might have a common origin.

---

[1]Composition, where up to 20 percent of the Cr atoms have be replaced by Mo.

[2]Microstucture, where, for example, in NiAl-33Cr-3Mo (fig. 7, (ref. 14)) and NiAl-31Cr-1Mo (ref. 16) transverse sections have revealed mm diameter planer eutectic grains without intercellular regions and ~200 μm diameter cells with ~20 μm thick intercellular regions.

[3] Second phase morphology (refs. 2 and 3), where DS NiAl-34Cr has Cr fibers in a NiAl matrix, while the Mo-modified versions are composed of alternating lamella of NiAl and α-(Cr,Mo).

[4] Growth directions (refs. 2 and 3), where NiAl and Cr in DS NiAl-34Cr have [001] growth axes and matching (100) planes, but NiAl and α-(Cr,Mo) in the Mo-modified versions have [111] growth axes and matching (refs. 11 and 2) interface planes.

Kollura and Pollock (ref. 17) have recently applied numerical analysis to model creep of DS NiAl-34Cr at 1273 K, and they basically concluded that creep parallel to the Cr fiber axis takes place by plastic deformation of the NiAl matrix which transfer load to elastic Cr fibers. As partial support for this mechanism, they calculated much higher creep rates than those measured in this eutectic if it was assumed that the Cr-fibers crept at a rate one hundredth of that for the NiAl matrix. Additionally, they cited transmission electron microscope (TEM) evidence (ref. 18) that shows (1) the Cr fibers were dislocation-free and (2) no substantial differences in the NiAl substructure existed between deformed NiAl-34Cr and single phase NiAl.

Their latter contention is at odds with other observations of substructure in NiAl deformed at elevated temperature, where, for example, it was demonstrated that doping NiAl with 0.09N will produce a distribution of AlN particles which can anchor a small subgrain structure (ref. 19). In fact the AlN particles forced the matrix to behave as a constant substructure material which was stronger than single phase NiAl and essentially followed the behavior predicted by Sherby, et al., (ref. 20) with a high stress exponent ($n \approx 8$) and activation energy near that for volume diffusion. If subgrains do develop in NiAl during the elevated deformation of DS NiAl-(Cr,Mo) eutectics, then the NiAl/α-(Cr,Mo) interfaces should act as pinning points which would force the subgrains to be of the same dimension as the lamella thickness (~1 μm, fig. 7) and lead to constant structure strengthening. In fact this was the conclusion of Jimenez, et al., (ref. 15) in NiAl-27Cr to account for an n = 8 regime, where 1.7 μm diameter Cr particles stabilized 1.5 μm diameter NiAl grains which restricted the subgrain size to ≤1.5 μm.

Since well developed subgrains have also been found in crept pure Cr (ref. 12), one could anticipate substructure strengthening via pining at Cr(Mo)/NiAl interfaces in the Cr fibers or α-(Cr,Mo) lamella. However, in view of Kolluru's observation of dislocation-free Cr fibers after 1273 K creep (ref. 17) and the absence of dislocations in 1.7 or 3.5 μm diameter Cr particles in NiAl-27Cr after elevated temperature deformation (ref. 15), this might not be the case. While the absence of dislocations in Cr was viewed to be evidence of elastic behavior (ref. 15 and 17), other interpretations of dislocation-free fibers/particles in the deformed materials are possible. For example if Cr offers very little resistance to dislocation motion within the fiber, once the dislocation is through the interface, it could quickly glide across and leave. The resistance to glide should be equal to the Orowan stress σ_o which is approximately Gb/l, where G is the shear modulus, b is the magnitude of the burgers vector and l is the fiber diameter/lamella thickness. From the G,b values for Cr given by Frost and Ashby (ref. 21) at 1300 K, σ_o = 24.3/l Pa•m which would range from about 8 MPa for a 3 micron diameter/spacing to 50 MPa for a 0.5 micron diameter/spacing. In view of the ~1.5 μm Cr-fibers diameter (refs. 3 and 4), the lamella thickness (fig. 7) and the 1300 K strength levels demonstrated for the DS NiAl-(Cr,Mo) eutectics in figure (9), the fibers/plates should not restrict glide. A similar conclusion can also be drawn for NiAl without an internal structure, where, from the G,b values for NiAl reported by Noebe, Bowmann and Nathal (ref. 22), the Orowan stress at 1300 K is given by σ_o = 15.7/l Pa•m which corresponds to ~5 MPa at a 3 micron spacing and 31 MPa at 0.5 microns.

The limitation of Cr-fibers to only elastic deformation during elevated temperature creep of DS NiAl-34Cr is also drawn into question by several other studies. Examination of 1200 to 1400 K compressive creep behavior of cryomilled NiAl containing about 10 vol % Cr (ref. 13) indicated that the strength of these composites followed the Rule-of-Mixtures, where Cr deformed at the rates described by Stephens and Klopp (ref. 12). A similar observation was made by Venkatesh and Dunand (ref. 23), who studied the elevated temperature compressive properties of continuous, unidirectional W-wires imbedded in NiAl, and they found that the creep strength of composites containing from 5 to 20 vol % W could be described by the Rule-of-Mixtures. Lastly by analogy to W wire, one would expect substructure free Cr-fibers to be relatively weak and prone to deformation since recrystallization of worked W-wires has been shown to severely reduce their creep strength (refs. 23 and 24).

Clearly, there is a need for detailed TEM studies of creep deformed directionally solidified NiAl-(Cr,Mo) eutectics to increase our understanding of deformation and strengthening in these materials. In reality, very little is known about dislocation structures in any of these alloys. To date the available information consists of the observation of an interfacial network of dislocations (refs. 3, 5, 25 and 26) to accommodate the semicoherent interface between NiAl and α-(Cr,Mo) in as-grown eutectics and the citation of no unusual substructure in NiAl nor dislocations in Cr-fibers in crept NiAl-34Cr (ref. 17). Any future effort to examine the behavior of DS NiAl-(Cr,Mo) at elevated temperature should include a commitment for a through TEM analysis.

SUMMARY OF RESULTS

Elevated temperature compressive flow strength–strain rate properties of Ni-33Al-31Cr-3 Mo between 1200 and 1400 K have been measured for alloys directionally solidified at rates ranging from 7.6 to 508 mm/h. All the eutectics possessed statistically alike strength levels except for the alloy grown at 25.4 mm/h which was slightly stronger. While the microstructure was dependent on the growth rate, no microstructual reason could be found for this improvement.

REFERENCES

1. J.L. Walter and H.E. Cline: *Metall. Trans.* **1,** (1970), pp. 1221–1229.
2. H.E. Cline and J.L. Walter: *Metall. Trans.* **1,** (1970), pp. 2907–2917.
3. D.R. Johnson, X.F. Chen, B.F. Oliver, R.D. Noebe, and J.D. Whittenberger: *Intermetallics* **3,** (1995), pp. 99–113.
4. T.M. Pollock and D. Kollura: Micromechanics of Advanced Materials, eds. S.N.G. Chu, P.K. Law, R.J. Arsenault, K. Sadananda, K.S. Chan, W.W. Gerberich, C.C. Chau, and T.M. Kung: TMS, Warrendale, PA, 1995, pp. 205–212.
5. J.M. Yang, S.M. Jeng, K. Bain, and R.A. Amato: *Acta Mater.* **45,** (1997), pp. 295–305.
6. J.D. Whittenberger, S.V. Raj, I.E. Locci, and J.A. Salem: *Intermetallics* **7,** (1999), pp. 1159–1168.
7. S.V. Raj, I.E. Locci, and J.D. Whittenberger: *Creep Behavior of Advanced Materials for the 21st Century* (edited by R.S. Mishra, A.K. Mukherjee, and K. Linga Murty), TMS, Warrendale, PA, 1999, pp. 295–310
8. S.V. Raj, I.E. Locci, and J.D. Whittenberger: 3rd International Symposium on Structural Intermetallics (ISSI-3), eds. K.J. Hemker, D.M. Dimiduk, H. Clemens, R. Darolia, H. Inui, J.M. Larsen, V.K. Sikka, M. Thomas, and J.D. Whittenberger: TMS, Warrendale, PA, 2001, pp. 785–794.
9. S. Walston and R. Darolia: 3rd International Symposium on Structural Intermetallics (ISSI-3), eds. K.J. Hemker, D.M. Dimiduk, H. Clemens, R. Darolia, H. Inui, J.M. Larsen, V.K. Sikka, M. Thomas, and J.D. Whittenberger: TMS, Warrendale, PA, 2001, pp. 735–744.
10. J.D. Whittenberger, *J. Mat. Sci.* **22**,(1987), pp. 394–402.
11. K.R. Forbes, U. Glatzel, R. Darolia, and W.D. Nix: *Metal. Mat. Trans.* A **27A,** (1996), pp. 1229–40.
12. J.R. Stephens and W.D. Klopp: *J. Less Com. Metals* **27**, (1972), pp. 87–94.
13. J.D. Whittenberger, Beverly Aikin, and Jon Salem: *J. Mater. Res.* **16,** (2001), pp. 1333–1344.
14. S.V. Raj and I.E. Locci: *Intermetallics* **9,** (2001), pp. 217–27.
15. J.A. Jimenez, S. Klaus, M. Carsi, O.A. Ruano, and G. Frommeyer: *Acta Mater*. **47** (1999), pp. 3655–3662.
16. J.D. Whittenberger, S.V. Raj, I. Locci, and J.A. Salem: submitted to *Metal. Mat. Trans. A*.
17. D.V. Kollura and T.A. Pollock: *Acta Mater*. **46**, (1998), pp. 2859–2876.
18. D. Kolluru: The creep deformation of directionally solidified NiAl-Cr and NiAl-Cr(Mo) eutectics. Ph.D. Thesis Carnegie Mellon University, Pittsburgh, PA, 1997.
19. J.D Whittenberger, R.D. Noebe, and A. Garg: *Metal. Mat. Trans. A* **27A**, (1996), pp. 3170–80.
20. O.D. Sherby, R.H. Klundt, and A.K. Miller: *Metal. Trans. A* **8A**, (1977), pp. 843–50.
21. H.J. Frost and M.F. Ashby: Deformation Mechanism Maps, 1982, Pergamon Press, NY, NY.
22. R.D. Noebe, R.R. Bowman, and M.V. Nathal: *Inter. Mater. Rev*. **38**, (1993), 193-232.
23. T.A. Venkatesh and D.C Dunand: *Metal. Mat. Trans. A* **31A** (2000) pp. 781–792.
24. J.W Pugh: *Metal. Trans*. **4**, (1973), pp. 533–538.
25. J.L. Walter, H.E. Cline, and E.F. Koch: *Trans. TMS-AIME*. **245**, (1969), pp. 2073–2079.
26. E.F. Koch, H.E. Cline, J.L. Walter, and L.M. Osika: *Acta Metall*. **19**, (1971), pp. 405–414.

TABLE I.—DESCRIPTIONS OF THE FLOW STRESS–STRAIN RATE–TEMPERATURE BEHAVIOR FOR AS-CAST AND DIRECTIONAL SOLIDIFIED Ni-33Al-31Cr-3Mo.

(a) Temperature compensated exponential law							
Growth velocity, mm/h	A, s^{-1}	C	δ_C	Q, kJ/mol	δ_Q	R_d^2	Date points not utilized in the analyses
7.6	2.93×10^{16}	0.0419	0.0021	–627.1	37.1	0.981	1200 K > $10^{-5}s^{-1}$
12.7	3.97×10^{11}	0.0307	0.0017	–480.4	34.1	0.974	1200 K – $10^{-4}s^{-1}$, 1300 K < $10^{-7}s^{-1}$ & 1400 K < $10^{-7}s^{-1}$
As Cast (12.7)	4.59×10^{5}	0.0391	0.0022	–326.7	30.3	0.973	
25.4	3.03×10^{14}	0.0363	0.0024	–582.3	49.7	0.966	1200 K > $10^{-5}s^{-1}$ and 1300 K – $10^{-3}s^{-1}$
50.8	5.96×10^{11}	0.0356	0.0014	–498.8	28.4	0.982	1400 K < $10^{-7}s^{-1}$
127	2.34×10^{11}	0.0331	0.0012	–490.4	22.2	0.988	1200 K –$10^{-4}s^{-1}$
254	1.31×10^{13}	0.0334	0.0013	-533.7	24.4	0.985	
508	2.06×10^{10}	0.0294	0.0018	-451.6	35.7	0.968	
(b) Temperature compensated power law							
Growth velocity, mm/h	A, s^{-1}	n	δ_n	Q, kJ/mol	δ_Q	R_d^2	Date points not utilized in the analyses
7.6	1.29×10^{4}	6.37	0.38	–588.2	38.0	0.977	1200 K > $10^{-5}s^{-1}$ and 1300 K – $10^{-3}s^{-1}$
12.7	9.21	4.43	0.20	–405.1	29.9	0.989	1200 K > $10^{-5}s^{-1}$, 1300 K > $10^{-4}s^{-1}$ and 1400 K – $10^{-3}s^{-1}$
As Cast (12.7)	0.714	4.83	0.33	–374.7	31.8	0.971	1200 K –$10^{-4}s^{-1}$ and 1300 K – 10^{-3} s^{-1}
25.4	3.05×10^{3}	5.61	0.18	–539.4	24.3	0.991	1200 K > $10^{-5}s^{-1}$ and 1300 K – $10^{-3}s^{-1}$
50.8	5.96×10^{1}	4.88	0.16	–450.0	22.4	0.989	1200 K > $10^{-5}s^{-1}$ and 1300 K – $10^{-4}s^{-1}$
127	1.47×10^{1}	4.53	0.35	–475.0	35.2	0.975	1200 K > $10^{-5}s^{-1}$
254	2.20×10^{3}	5.58	0.42	–531.2	39.9	0.965	1200 K > $10^{-5}s^{-1}$ and1300 K – $10^{-3}s^{-1}$
508	4.27	5.58	0.41	–460.1	34.7	0.969	1200 K – $10^{-4}s^{-1}$ and 1300 K – $10^{-3}s^{-1}$

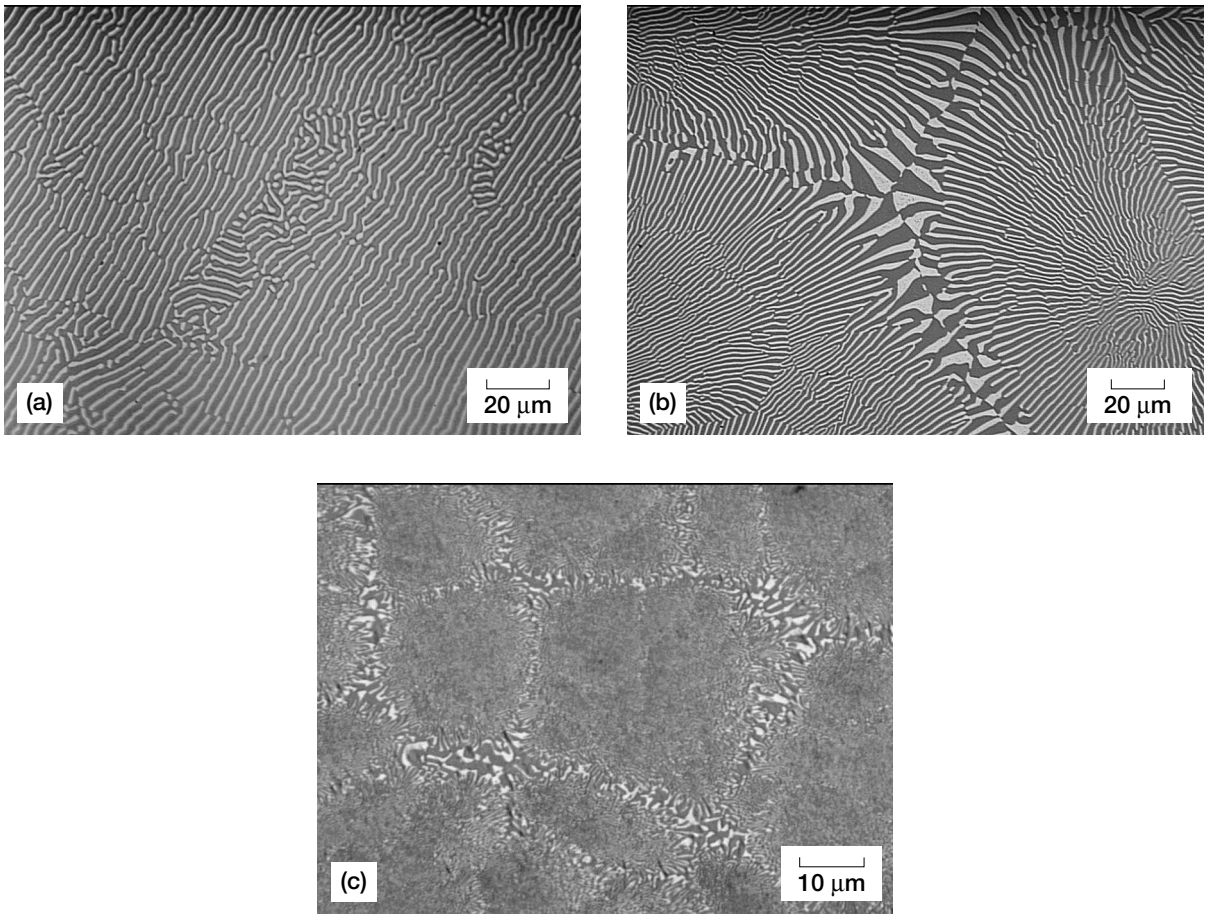

Figure 1.—Transverse light optical, unetched microstructures of the eutectic alloys. (a) Ni-33.3Al-31.2Cr-2.9Mo directionally solidified at 7.6 mm/h, (b) Ni-33.9Al-30.8Cr-2.9Mo directionally solidified at 50.8 mm/h and (c) as-cast Ni-33.3Al-31.1Cr-3.0Mo.

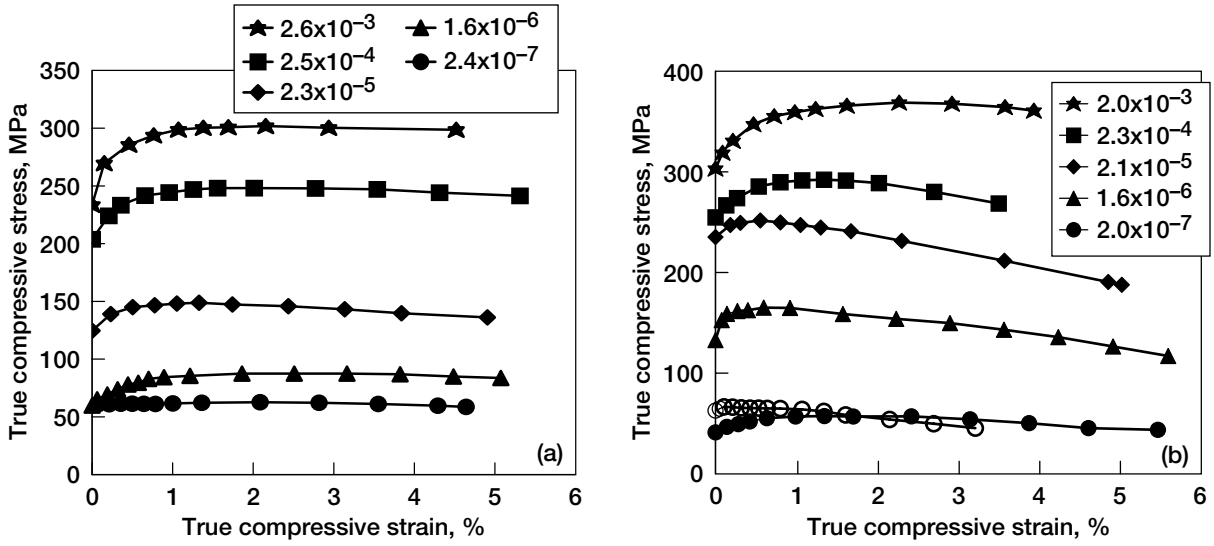

Figure 2.—Typical true compressive stress-strain curves for Ni-33Al-31Cr-3Mo at 1300 K obtained via constant velocity testing at 1300 K as a function of the nominally imposed strain rate. (a) as-cast Ni-33.3Al-31.1Cr-3.0Mo and (b) Ni-33.0Al-32.2Cr-3.0Mo directionally solidified at 12.7 mm/h, where the set of open and filled symbols represent data from near duplicate test conditions.

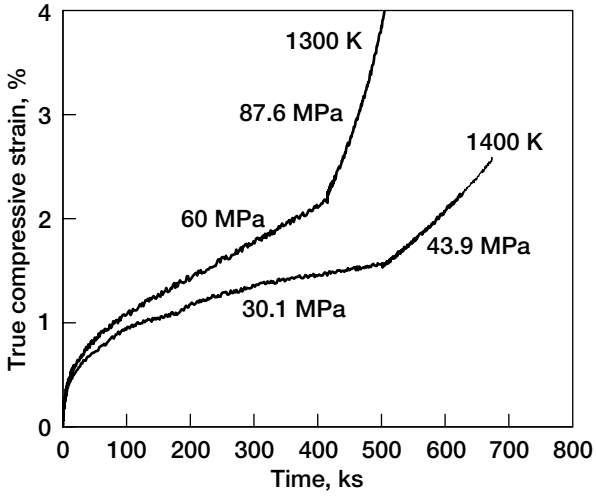

Figure 3.—Typical 1300 K and 1400 K compressive creep curves as a function of engineering stress for Ni-33.9Al-30.8Cr-2.9Mo directionally solidified at 50.8 mm/h.

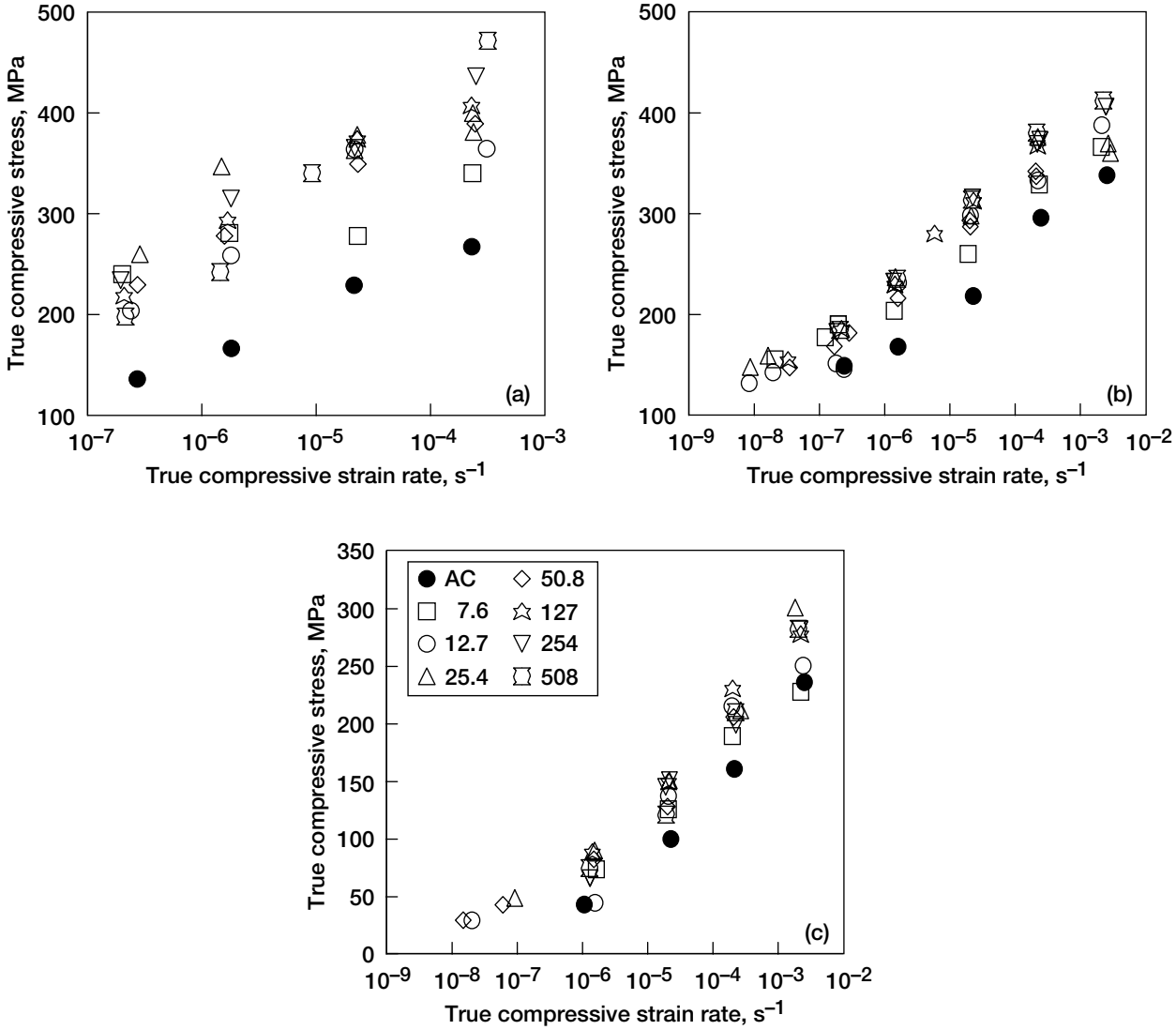

Figure 4.—True compressive flow stress-strain rate behavior for Ni-33Al-31Cr-3Mo as a function of the directionally solidification growth rate at (a) 1200 K, (b) 1300 K and (c) 1400 K.

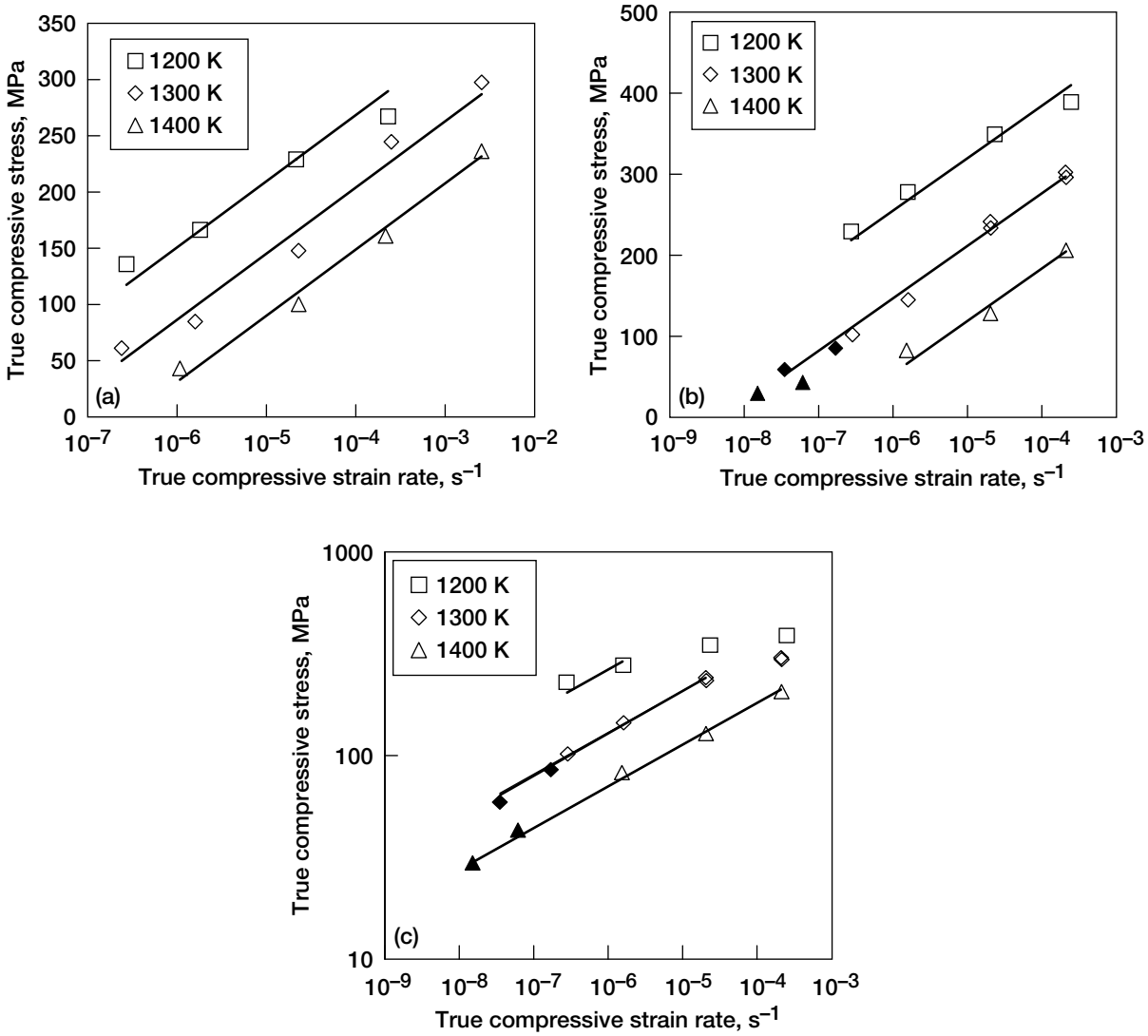

Figure 5.—True compressive flow stress-strain rate-temperature behavior for (a) as-cast Ni-33.3Al-31.1Cr-3.0Mo and (b,c) Ni-33.9Al-30.8Cr-2.9Mo directionally solidified at 50.8 mm/h. Data points from constant velocity testing are shown as open symbols, while constant load creep test results are given as solid symbols.

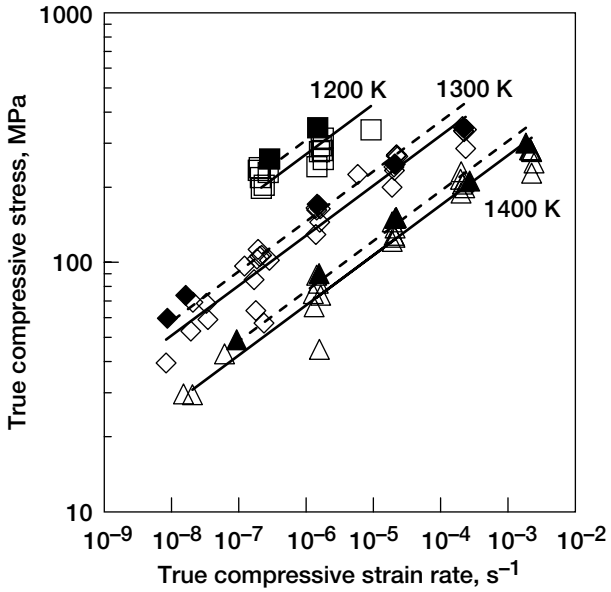

Figure 6.—Comparison of the true compressive flow stress-strain rate-temperature properties of Ni-33Al-31Cr-3Mo directionally solidified at 7.6, 12.7, 50.8, 127, 254, and 508 mm/h (open symbols) with those for the alloy grown at 25.4 mm/h (filled symbols).

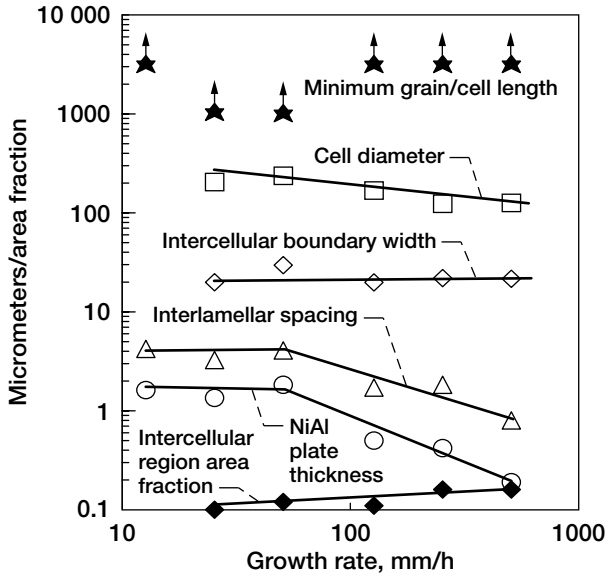

Figure 7.—Estimated grain/cell lengths, average cell diameter, intercellular region width, interlamellar spacing, NiAl plate thickness and area fraction of the intercellular region for directional solidified Ni-33Al-31Cr-3Mo as a function of growth rate. Intercellular regions were not formed in the alloys directionally solidified at 7.6 and 12.7 mm/h and the grain diameters for these two conditions were > 1 mm.

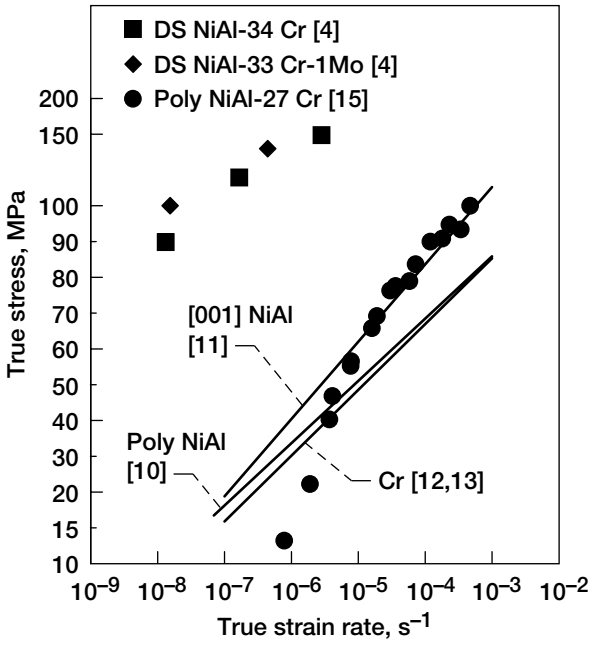

Figure 8.—Comparison of the 1273 K flow stress-strain rate properties of several directionally solidified NiAl-34Cr based eutectics to those for single-and polycrystalline NiAl, polycrystalline Cr and a two phase polycrystalline NiAl-27Cr mixture.

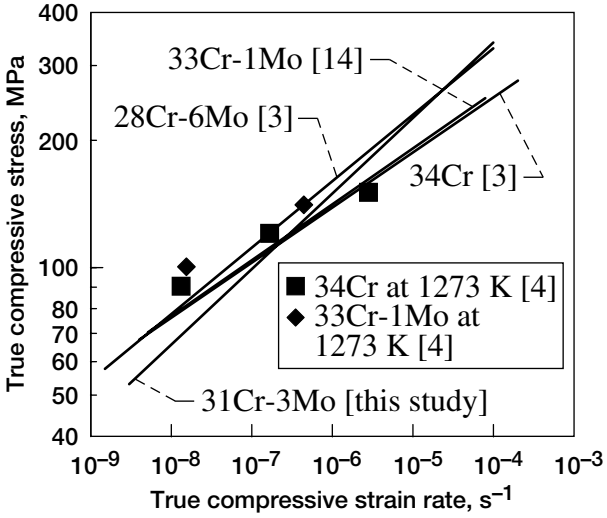

Figure 9.—Comparison of the compressive flow stress-strain rate properties of several directionally solidified NiAl-34Cr based eutectics with/without Mo additions at/near 1300 K.

REPORT DOCUMENTATION PAGE

Form Approved
OMB No. 0704-0188

1. AGENCY USE ONLY (*Leave blank*)	2. REPORT DATE	3. REPORT TYPE AND DATES COVERED
	December 2001	Technical Memorandum

4. TITLE AND SUBTITLE

Effect of Microstructure on Creep in Directionally Solidified NiAl-31Cr-3Mo

5. FUNDING NUMBERS

WU–708–31–13–00

6. AUTHOR(S)

J.D. Whittenberger, S.V. Raj, and I.E. Locci

7. PERFORMING ORGANIZATION NAME(S) AND ADDRESS(ES)

National Aeronautics and Space Administration
John H. Glenn Research Center at Lewis Field
Cleveland, Ohio 44135–3191

8. PERFORMING ORGANIZATION REPORT NUMBER

E–13007

9. SPONSORING/MONITORING AGENCY NAME(S) AND ADDRESS(ES)

National Aeronautics and Space Administration
Washington, DC 20546–0001

10. SPONSORING/MONITORING AGENCY REPORT NUMBER

NASA TM—2001-211306

11. SUPPLEMENTARY NOTES

Prepared for the 131st Annual Meeting and Exhibition sponsored by the Minerals, Metals, and Materials Society, Seattle, Washington, February 17–21, 2002. J.D. Whittenberger and S.V. Raj, NASA Glenn Research Center, and I.E. Locci, Case Western Reserve University, Cleveland, Ohio 44106. Responsible person, J.D. Whittenberger, organization code 5120, 216–433-3196.

12a. DISTRIBUTION/AVAILABILITY STATEMENT

Unclassified - Unlimited
Subject Category: 26 Distribution: Nonstandard

Available electronically at http://gltrs.grc.nasa.gov/GLTRS

This publication is available from the NASA Center for AeroSpace Information, 301–621–0390.

12b. DISTRIBUTION CODE

13. ABSTRACT ***(Maximum 200 words)***

The 1200 to 1400 K slow strain rate characteristics of the directionally solidified (DS) eutectic Ni-33Al-31Cr-3 Mo have been determined as a function of growth rate. While differences in the light optical level microstructure were observed in alloys grown at rates ranging from 7.6 to 508 mm/h, compression testing indicated that all had essentially the same strength. The exception was Ni-33Al-31Cr-3Mo DS at 25.4 mm/h which was slightly stronger than the other growth velocities; no microstructural reason could be found for this improvement. Comparison of the ~1300 K properties revealed that four different DS NiAl-34(Cr,Mo) alloys have a similar creep resistance which suggests that there is a common, but yet unknown, strengthening mechanism.

14. SUBJECT TERMS	15. NUMBER OF PAGES
Nickel aluminides; Mechanical properties; Elevated temperature; Directional solidification; NiAl-(Cr,Mo) eutectic	19
	16. PRICE CODE

17. SECURITY CLASSIFICATION OF REPORT	18. SECURITY CLASSIFICATION OF THIS PAGE	19. SECURITY CLASSIFICATION OF ABSTRACT	20. LIMITATION OF ABSTRACT
Unclassified	Unclassified	Unclassified	